IOPscience iopscience.iop.org

Home Search Collections Journals About Contact us My IOPscience

Application of nanosecond-pulsed dielectric barrier discharge for biomedical treatment of topographically non-uniform surfaces

This content has been downloaded from IOPscience. Please scroll down to see the full text.

2009 J. Phys. D: Appl. Phys. 42 125202

(http://iopscience.iop.org/0022-3727/42/12/125202)

View the table of contents for this issue, or go to the journal homepage for more

Download details:

IP Address: 144.118.183.94
This content was downloaded on 07/08/2014 at 15:17

Please note that terms and conditions apply.

IOP PUBLISHING JOURNAL OF PHYSICS D: APPLIED PHYSICS

J. Phys. D: Appl. Phys. **42** (2009) 125202 (5pp) doi:10.1088/0022-3727/42/12/125202

Application of nanosecond-pulsed dielectric barrier discharge for biomedical treatment of topographically non-uniform surfaces

H Ayan[1], D Staack[1], G Fridman[2], A Gutsol[3], Y Mukhin[1], A Starikovskii[1], A Fridman[1] and G Friedman[4]

[1] Department of Mechanical Engineering and Mechanics, College of Engineering, Drexel University, Philadelphia, PA 19104, USA
[2] School of Biomedical Engineering, Science, and Health Systems, Drexel University, Philadelphia, PA 19104, USA
[3] Chevron Energy Technology Company, Richmond, CA 94802, USA
[4] Department of Electrical and Computer Engineering, College of Engineering, Drexel University, Philadelphia, PA 19104, USA

Received 17 November 2008, in final form 31 March 2009
Published 22 May 2009
Online at stacks.iop.org/JPhysD/42/125202

Abstract
Antimicrobial effectiveness of a nanosecond-pulsed dielectric barrier discharge (DBD) was investigated and compared with that of a microsecond-pulsed DBD. Experiments were conducted on the *Escherichia coli* bacteria covering a topographically non-uniform agar surface acting as one of the DBD electrodes. They reveal that the nanosecond-pulsed DBD can inactivate bacteria in recessed areas whereas the microsecond-pulsed and conventional DBDs fail to do so. Charged species (electrons and ions) appear to play the major role in the bacteria inactivation with the nanosecond-pulsed DBD. Moreover, the nanosecond-pulsed DBD kills bacteria significantly faster than its microsecond-pulsed counterpart.

(Some figures in this article are in colour only in the electronic version)

1. Introduction

It has been demonstrated recently that direct treatment of relatively smooth surfaces and living tissues by non-thermal dielectric barrier discharge (DBD) in air is highly effective in killing bacteria and fungi [1, 2] that colonize these surfaces. The key aspect of the direct treatment was shown to be contact with electrical charges. When most of the charges were separated from the treatment area by a metal mesh, the observed pathogen deactivation rates were much slower suggesting that UV or long living species such as ozone alone have a much weaker effect [3, 4]. These results hold significant promise for medical applications such as sterilization of wound surfaces. However, a typical DBD in air can be highly non-uniform [5–7], particularly on topographically non-uniform surfaces such as most of the living tissues. Microdischarges within the DBD can be pinned to 'ridges' on skin, for example, delivering charge to the surface in a highly non-uniform manner. As a result, it is not clear that pathogens can be destroyed as effectively on the recessed areas between the ridges of real tissue by the conventional DBD in air.

In this study we investigate the effectiveness of a DBD excited by nanosecond rise and fall time voltage pulses in killing bacteria covering topographically non-uniform surfaces. Experiments were conducted on the bacteria covered agar surface acting as one of the DBD electrodes. The nanosecond-pulsed DBD was tested on non-uniform surfaces and produced uniform plasma independent of the surface topography and demonstrated complete bacteria inactivation. Although results reported here relate to surface disinfection, many of the conclusions can be extended to other types of treatments of topographically non-uniform surfaces. In addition, although several investigators did report uniform

 © 2009 IOP Publishing Ltd Printed in the UK

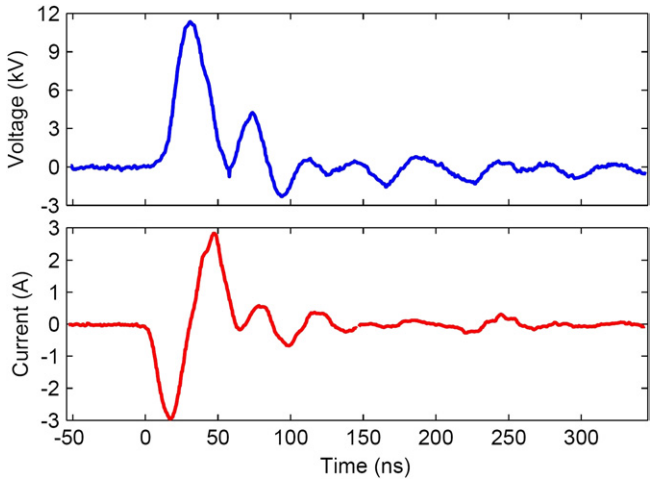


Figure 1. Typical voltage and current waveforms of nanosecond-pulsed DBD.

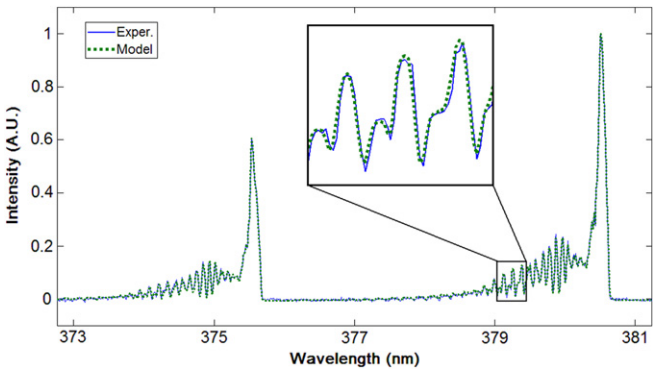


Figure 2. Experimental spectrum and simulated spectrum of nanosecond-pulsed DBD ($T_{rot} = 313.5 \pm 7.5$ K and $T_{vib} = 3360 \pm 50$ K).

DBD type discharges, to our knowledge the uniform discharge reported here is the only one to have been demonstrated at atmospheric pressure in open moist air over topographically non-uniform surfaces.

2. Experimental setup

2.1. Discharge characteristics

A typical oscilloscope (TDS5052B, Tektronix, Inc., TX) trace of the nanosecond-pulsed DBD applied voltage is given in figure 1. In addition to the electrical characterization, emission spectroscopy was employed to measure the vibrational and rotational temperatures (T_{vib} and T_{rot}) of the DBD using 375.4 and 380.4 nm vibrational lines and rotational structure in this region of the second positive system of molecular nitrogen, N_2 ($C^3\Pi_u$–$B^3\Pi_g$). T_{vib} and T_{rot} were determined by the best fit (minimum RMSE) between the modelled and experimental spectrum (figure 2) described in detail elsewhere [8]. Rotational and vibrational temperatures were measured to be 313.5 ± 7.5 K and 3360 ± 50 K respectively, for the power range that has been used for the experiments explained below. These 'temperatures' describe the relative population of different vibrational and rotational levels of the C^3 state of molecular nitrogen. Rotational distribution of the C^3 state under the pulsed excitation at high overvoltage reflects the rotational population of the ground state and gives information on the translational temperature of the gas. Vibrational spectra of the second positive system cannot be directly associated with vibrational or translational temperatures of molecules. This distribution reflects the interplay between the population by e-impact from different lower states and depopulation due to the collisional quenching and radiative processes. Thus the vibrational distribution is a qualitative indicator of the electron's temperature in the discharge region. Thus we have demonstrated that the nanosecond-pulsed DBD does not heat the gas but provides strong excitation of the gas due to the high energy of the electrons.

The experimental setup and the high voltage electrode that has been employed in antimicrobial treatment experiments are presented in figure 3(*a*). Figure 3(*d*) is a schematic of the setup with a partial cross-sectional view of the high voltage electrode. The planar high voltage electrode consists of a 10 mm diameter copper core insulated by a layer of quartz that has 0.66 mm thickness and is located 0.5 mm above the top of the treatment surface by spacers. Counter electrode is the agar dish placed on a conducting substrate.

2.2. Agar plates

In general, two different types of agar plates were used for experiments. The first type of agar was made out of water and broth (Difco Brain Heart Infusion Agar powder, Fisher Scientific, PA) mixture that solidifies shortly after it is poured into the Petri dish with a plain surface. These planar surfaces were used as controls and also in the studies of non-uniform surfaces by placing meshes over them. The agar plates of the second type were specially prepared to have non-uniform surfaces (with ridges and indentations) on the agar to mimic the real case for living skin tissue. The topographical features on the agar were moulded by placing polymer (PTFE) forms at the bottom of the dish prior to adding the agar and then inverting the agar and removing the form after solidification. The agar shown in figure 3(*a*) is an example of this second type that was patterned with a three-level recess with 2 mm width and 0.33 mm depth at every stage.

2.3. Bacteria preparation

Escherichia coli bacteria (*E. coli* K12 strain, Ward's Natural Science, Rochester, NY) were plated onto the surface of agar at concentrations of 10^8 CFUs ml^{-1} (colony forming units per millilitre). The suspension volume (water and bacteria) was 2 ml to maintain full coverage over the entire surface of the agar. Concentrations were measured and calculated by a standard dilution assay on the smooth agar plates [3]. Before plasma treatment the bacteria seeded plates were left to dry in the laminar flow hood for one and a half hours. After plasma treatment, treated and untreated (control) samples were cultured for 12 h in the incubator at 37 °C. Inactivation results were evaluated by visually examining the resulting colonies after incubation. After 12 h of incubation, *E. coli* colonization

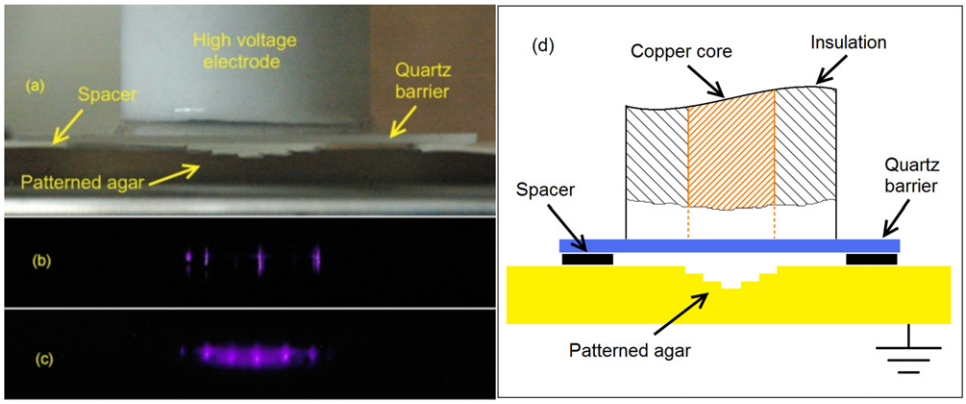


Figure 3. Side view of (*a*) high voltage electrode with no plasma, (*b*) conventional microsecond-pulsed DBD, (*c*) nanosecond-pulsed DBD on the patterned agar surface and (*d*) schematic of the experimental setup (pictures of discharges were taken with 0.5 s exposure time (60 pulses) for both systems and schematic is not to scale).

becomes visible. Pictures were taken after 12 h of incubation. Samples were also observed up to 48 h incubation and delayed recovery was not found in the plasma treated regions.

3. Experimental results

3.1. DBD images

For the experiments the high voltage electrode was powered by two distinct power supplies. The main focus of the study is the system with nanosecond rise and fall time voltage pulses which produced a uniform DBD [9]. The plasma source is composed of two segments: a current source and a double spark gap circuit. When the source charges the capacitor, the first spark gap breaks down and the charge stored in the capacitor is transferred to the discharge. Voltage across the plasma gap rises rapidly until the second spark gap discharges and shorts outs the plasma gap. The result is a rapid decay of the voltage across the plasma gap. Characteristics of the nanosecond pulses are as follows: 20 ns duration, 13 kV amplitude, ~3 kV ns^{-1} rise/fall rate, 120 Hz frequency. On the other hand, we have compared the antimicrobial effectiveness of nanosecond-pulsed DBD with that of a more conventional DBD system. This second discharge was generated by employing microsecond rise and fall time voltage pulses which resulted in a conventional non-uniform DBD. Microsecond-pulsed DBD was generated by 1.5 μs long, 10 kV pulses with a 20 V ns^{-1} voltage rise rate at 120 Hz. In all experiments with both systems, the average power density for the active area of the high voltage electrode was kept at the level of 100 mW cm^{-2} that is approximately 75 mW power for 1 cm electrode diameter.

In the previous section, in figure 3, the side view of the high voltage electrode on the patterned agar surface (figure 3(*a*)), and the typical appearance of a conventional microsecond-pulsed DBD (figure 3(*b*)) and a nanosecond-pulsed DBD (figure 3(*c*)) are given. A two-piece spacer with 0.5 mm thickness was placed between the high voltage electrode and the top surface of the agar (figure 3(*d*)). The figure presents a clear distinction between the discharges. The nanosecond-pulsed DBD produces a relatively uniform plasma that fully covers the entire gap (a glow with bright spots over the sharp corners), whereas the conventional DBD produces only microdischarges (filaments) that were often terminated on the top of asperities and irregularities.

3.2. Bacteria inactivation results with mesh on agar

The first part of the experiments was done by placing a stainless steel mesh over the smooth surface agar. In this case the metal mesh simulated the effects of the ridges and indentations, i.e. the surface non-uniformities. The openings between the wires of the mesh are 1.5 mm, the wires are 0.25 mm in diameter and the total thickness of the mesh is 0.5 mm. The gap between the bottom of the quartz insulation of the high voltage electrode and the top of the mesh was 1 mm.

A typical inactivation result comparing both DBDs and a schematic side view of the setup are shown in figure 4. Light colour areas in figure 4(*a*) are the locations on the agar where complete inactivation by 30 s plasma treatment occurred, while the rest of the agar with a darker colour remains *E. coli* covered (10^8 CFU ml^{-1}). On the left-hand side of this figure, inactivation was achieved within the 'valleys' and with a slightly larger diameter than the active area of the high voltage electrode. In contrast, conventional DBD affects a significantly smaller area (on the right-hand side of figure 4(*a*)). These preliminary results from the experiments clearly indicated that the nanosecond-pulsed discharge is much more effective and faster than the conventional microsecond-pulsed DBD in killing *E. coli* bacteria.

3.3. Bacteria inactivation results with patterned agar

The antimicrobial effect of DBDs has also been tested on the aforementioned three-level recess patterned agar plates whose cross-sectional view is given in figure 3. Prior to the experiments described in this study, uniform distribution of bacteria on the patterned surfaces was verified with a separate experiment by pipetting low enough concentrations (10^3–10^4 CFU ml^{-1}) to get a countable number of colonies on the surface.

In figure 5 the difference in the performance of two different discharges can be easily seen. In the case

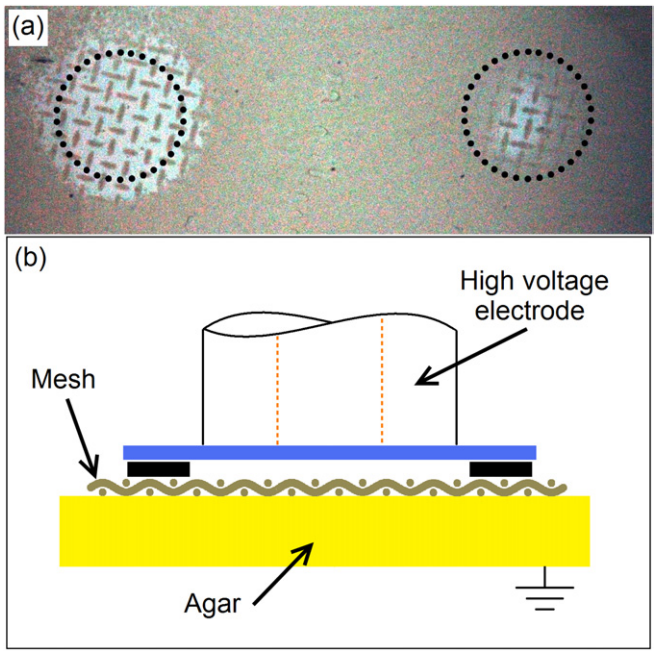


Figure 4. (*a*) Inactivation with nanosecond- (left-hand side) and microsecond- (right-hand side) pulsed DBD through metal mesh and (*b*) schematic of the experimental setup (schematic is not to scale; circles in (*a*) indicate the edge of the high voltage electrode; brightness and contrast of the image were adjusted for clarity, no other modifications done).

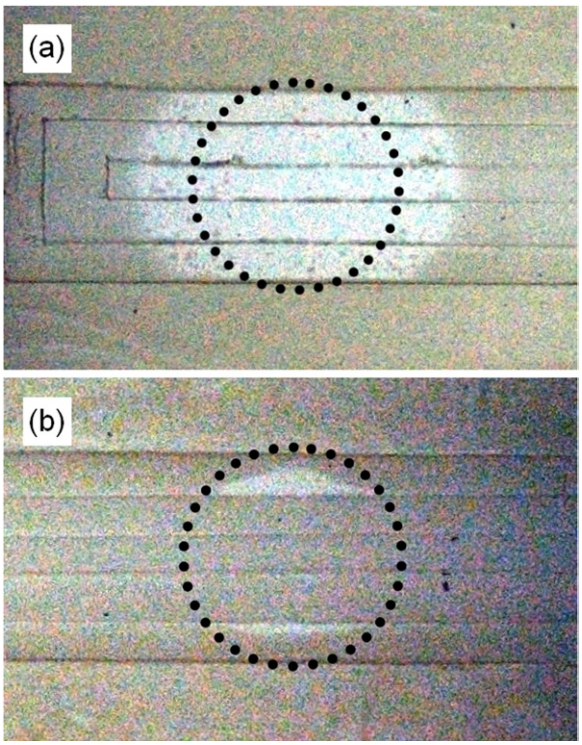


Figure 5. Three-level recessed agar surface treated with (*a*) nanosecond-pulsed DBD and (*b*) microsecond-pulsed DBD. The width of each level (distance between the horizontal lines) is approximately 2 mm. For both plates, treatment time: 30 s, *E. coli* concentration: 10^8 CFU ml^{-1}. Circles indicate the edge of the high voltage electrode (brightness and contrast of the images were adjusted for clarity, no other modifications done).

of nanosecond-pulsed DBD all three levels are uniformly treated and bacteria inactivated (figure 5(*a*)) whereas in the case of conventional microsecond-pulsed DBD only partial disinfection is achieved in the vicinity of the edge of the first level where the discharge gap is minimal (figure 5(*b*)).

3.4. Mechanism of bacteria inactivation

In order to help understand the basic mechanism of bacteria inactivation with nanosecond-pulsed DBD, a single step recessed agar was used. The depth and the width of the recess were 0.66 mm and 10 mm, respectively. In the first case (figure 6(*a*)) there was no flow and the surface of the agar plates were treated for 30 s. In the second case (figure 6(*b*)), air was blown through the gap between the quartz and the bottom of the recess with 3 SLPM flow yielding approximately 7.5 m s^{-1} velocity at this cross-section. The results are similar to each other except for slight differences in the size of the inactivation area. However there is no qualitative difference between air flow and no flow cases, i.e. there is no afterglow effect at downstream of the flow (to the right-hand side of the figure). Lack of major differences in the two figures indicates that the bacteria inactivation occurs through direct contact with the plasma. The antimicrobial agents cannot be blown or translated away from the high voltage electrode location with air flow.

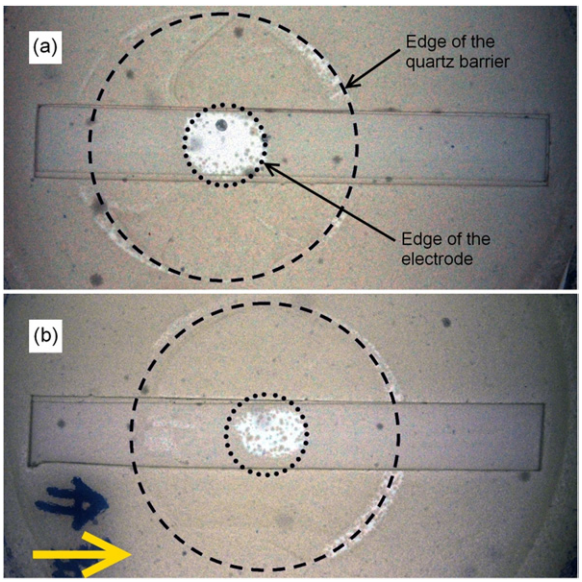


Figure 6. 30 s treatment with nanosecond-pulsed DBD (*a*) without air flow, and (*b*) with 3 SLPM air flow on single level recessed agar. Arrow in (*b*) indicates the direction of the flow.

It has been demonstrated previously that UV in atmospheric pressure DBD in air plays only a minor role in bacterial inactivation [3]. Since most of the charged particles remain in the plasma region (lifetime of charged particles at atmospheric pressures is very short) and the afterglow of the plasma contains mainly neutral atoms and molecules, [3, 4, 19] we conclude that bacteria inactivation using a nanosecond-pulsed DBD is mostly due to short living species including the charged particles.

4. Uniformity of nanosecond-pulsed discharge and discussion

Streamer formation and filamentary micro-structure are well-known features of traditional DBD [10, 11]. It is known, however, that uniformity of DBD plasma could be improved in two ways: (1) by increasing uniform pre-ionization of the gas and/or (2) shortening the voltage rise time [12]. In our case fast rise ($dV/dt > 1\,\mathrm{kV\,ns^{-1}}$) [13] of the applied voltage is the main factor responsible for the discharge uniformity [14, 15].

On the phenomenological level, transition from conventional non-uniform DBD to a uniform DBD can be explained using a simple time-scale analysis. Indeed, avalanches and subsequent streamers occur over very short time. This time can be roughly estimated on the basis of avalanche development. Given the maximum applied voltage of about 13 kV over a 1 mm gap, the reduced electric fields (E/n, where n is the gas concentration) is about $\sim 4 \times 10^{-15}\,\mathrm{V\,cm^2}$. This gives an electron drift velocity (v_d) in air of $\sim 10^7\,\mathrm{cm\,s^{-1}}$ [16] and a time of $\sim 10^{-8}\,\mathrm{s} = 10\,\mathrm{ns}$ to bridge a 1 mm gap. This time is the characteristic time of build-up of possible local non-uniformities in the electric field within the discharge gap.

If the voltage rise time is shorter than the time needed to bridge the gap and the maximum voltage significantly exceeds the critical breakdown voltage (discharge develops under high overvoltage conditions) the discharge develops uniformly due to the high electric field in front of the ionization wave. The high value of the reduced electric field E/n means: (1) suppression of the instabilities by saturation of the ionization coefficient; (2) fast expansion of the plasma channels and their overlapping; (3) generation of VUV-radiation and photoionization of the gas ahead of the ionization front; (4) generation of run-away electrons and pre-ionization of the gas [17]. Thus the criteria of the uniform discharge development could be formulated as simple relations:

$$(U/n)/h \gg (E/n)_{\mathrm{crit}} \tag{1}$$

and

$$\tau_{\mathrm{rise}} \ll h/v_{\mathrm{d}}, \tag{2}$$

where U is the maximal pulse voltage, n the gas density, h the discharge gap length, τ_{rise} the pulse rise time and v_{d} the electron's drift velocity in critical electric field [18].

For our conditions of DBD development we have: $(U/n)/h = 4 \times 10^{-15}\,\mathrm{V\,cm^2} \approx 3(E/n)_{\mathrm{crit}}$, $v_{\mathrm{d}} \sim 10^7\,\mathrm{cm\,s^{-1}}$, $\tau_{\mathrm{rise}} \sim 10\,\mathrm{ns}$ and critical voltage increase rate about $dV/dt \approx 1\,\mathrm{kV\,ns^{-1}}$. Thus the pulse used in this work with the high voltage increase rate of $dV/dt \approx 3\,\mathrm{kV\,ns^{-1}}$ generates a uniform plasma.

5. Conclusion

In summary, we have compared antimicrobial effectiveness of a nanosecond-pulsed DBD with a microsecond-pulsed DBD. Experiments reveal that the nanosecond-pulsed DBD inactivates bacteria over a larger surface area than the microsecond-pulsed DBD does for the same duration and power level. Moreover, experiments on non-uniform surfaces using meshes and patterned agars show that the nanosecond-pulsed DBD can penetrate into the recessed areas whereas the microsecond-pulsed DBD fails to do so. Nanosecond-pulsed DBD with short rise time and high overvoltage is insensitive to the morphological non-uniformities of the agar. Thus DBDs with nanosecond rise times are potentially more convenient for *in vivo* and hospital sterilization cases where the surfaces have non-uniform profiles. Additionally, experiments that have been conducted in order to understand the basic mechanism of bacteria inactivation by direct plasma, where charges come in contact comparing direct and indirect plasma effect, indicated that electrical charges play a major role in bacteria inactivation with nanosecond-pulsed DBD.

References

[1] Fridman A 2008 *Plasma Chemistry* (New York: Cambridge University Press) p 859

[2] Fridman G, Peddinghaus M, Ayan H, Fridman A, Balasubramanian M, Gutsol A, Brooks A and Friedman G 2006 *Plasma Chem. Plasma Process.* **26** 425–42

[3] Fridman G, Brooks A D, Balasubramanian M, Fridman A, Gutsol A, Vasilets V N, Ayan H and Friedman G 2007 *Plasma Process. Polym.* **4** 370–5

[4] Deng X, Shi J and Kong M G 2006 *IEEE Trans. Plasma Sci.* **34** 1310–6

[5] Fridman A and Kennedy L 2004 *Plasma Physics and Engineering* (New York: Taylor and Francis)

[6] Kogelschatz U 2003 *Plasma Chem. Plasma Process.* **23** 1–46

[7] Kogelschatz U 2002 *IEEE Trans. Plasma Sci.* **30** 1400–8

[8] Staack D, Farouk B, Gutsol A F and Fridman A A 2006 *Plasma Sources Sci. Technol.* **15** 818–27

[9] Ayan H, Fridman G, Gutsol A F, Vasilets V N, Fridman A and Friedman G 2008 *IEEE Trans. Plasma Sci.* **36** 504–8

[10] Fridman A, Chirokov A and Gutsol A 2005 *J. Phys. D: Appl. Phys.* **38** R1–R24

[11] Kozlov K V, Wagner H-E, Brandenburg R and Michel P 2001 *J. Phys. D: Appl. Phys.* **34** 3164–76

[12] Starikovskaia S M, Anikin N B, Pancheshnyi S V, Zatsepin D V, Starikovskii A Yu 2001 *Plasma Sources Sci. Technol.* **10** 344–55

[13] Roupassov D, Nudnova M, Nikipelov A, Starikovskii A 2008 *46th AIAA Aerospace Sciences Meeting and Exhibit (Reno, NV, USA)* AIAA 2008-1367

[14] Qi B, Ren C, Wang D, Li S-Z, Wang K and Zhang Y 2006 *Appl. Phys. Lett.* **89** 131503

[15] Choi J H, Han M H and Baik H K 2008 *Japan. J. Appl. Phys.* **47** 1071–5

[16] Dutton J 1975 *J.Phys. Chem. Ref. Dat.* **4** 577-856

[17] Levatter J I and Lin S-C 1980 *J. Appl. Phys.* **51** 210–22

[18] Zatsepin D V, Starikovskaia S M and Starikovskii A Yu 1998 *J. Phys. D: Appl. Phys.* **31** 1118

[19] Moisan M, Barbeau J, Crevier M-C, Pelletier J, Philip N and Saoudi B 2002 *Pure Appl. Chem.* **74** 349–58